

PHOTOCATALYTIC ACTIVITY OF ZnO-Ag NANOCOMPOSITES PREPARED BY A ONE-STEP PROCESS USING FLAME PYROLYSIS

K. Kusdianto^{1**}, W. Widiyastuti¹, Manabu Shimada², Tantular Nurtono¹, Siti Machmudah¹, Sugeng Winardi^{1*}

¹*Department of Chemical Engineering, Institut Teknologi Sepuluh Nopember (ITS), Kampus ITS, Sukolilo, Surabaya 60111, Indonesia*

²*Department of Chemical Engineering, Graduate School of Engineering, Hiroshima University, 4-1, Kagamiyama 1-chome, Higashi-Hiroshima, Hiroshima 739-8527, Japan*

(Received: July 2018 / Revised: October 2018 / Accepted: April 2019)

ABSTRACT

The degradation of organic pollutants using photocatalysis is more effective than conventional methods, with ZnO being the most widely used of the various semiconductor materials for application in photocatalysis. Unfortunately, degradation efficiency is inhibited by the electron-hole recombination. The photocatalytic activity of ZnO can be enhanced by adding noble metals, such as Ag nanoparticles. However, the fabrication of ZnO-Ag using liquid-phase processes is complicated and often requires multiple steps. In this study, the effects of Ag content, ranging from 0 to 20 wt%, in the photocatalytic activity of ZnO-Ag nanocomposites are investigated. The nanocomposites were fabricated by a one-step process using flame pyrolysis and with zinc acetate and AgNO₃ as the precursors. The nanocomposites were collected using an electrostatic precipitator and characterized by X-ray diffraction (XRD), scanning electron microscopy (SEM), and nitrogen adsorption-desorption of the Brunauer-Emmett-Teller (BET) specific surface area. The XRD results confirm the existence of Ag nanoparticles in the prepared nanocomposites, whose crystallite size was not significantly influenced by the presence of the nanoparticles. The SEM indicated that the morphology of the nanocomposites produced was spherical, with some aggregates. Particle size distribution of the nanocomposites increased with higher Ag content. The photocatalytic activity of the produced nanocomposites, estimated by evaluating the degradation of the methylene blue aqueous solution under UV irradiation, showed that the highest photocatalytic performance was attained when the concentration of Ag was equal to 5 wt%.

Keywords: Ag content; Gas-phase; Methylene blue degradation; Nanocomposite

1. INTRODUCTION

Organic pollutants from waste water can be degraded in several ways, such as adsorption, oxidation, reduction and photocatalysis (Balu et al., 2018; Kusrini et al., 2018; Mamat et al., 2018). The application of photocatalysis using semiconductor materials is reported to be more effective than the conventional chemical oxidation methods for degradation of these pollutants (Chatterjee & Dasgupta, 2005).

ZnO is the most widely used of the various semiconductor materials for application in photocatalysis due to its suitable band gap, non-toxicity, high chemical stability, cost-

*Corresponding author's email: swinardi@chem-eng.its.ac.id, Tel. +62-315946240, Fax. +62-315999282

** Corresponding author's email: kusdianto@chem-eng.its.ac.id, Tel. +62-315946240, Fax. +62-315999282
Permalink/DOI: <https://dx.doi.org/10.14716/ijtech.v10i3.2902>

effectiveness, strong oxidation ability, and easy availability (Duan et al., 2010). However, electron-hole recombinations inhibit the photocatalytic activity of pristine ZnO. Therefore, many attempts have been made to enhance the photocatalytic performance, such as by modification of the ZnO structure in order to increase the surface area and light absorption (Kadam et al., 2018). Furthermore, doping the ZnO nanoparticles with noble metals (Dermenci et al., 2014), lanthanide groups (Vaiano et al., 2017), natural zeolite (Rahman et al., 2018), and Fe₃O₄ (Winatapura et al., 2016) have also been reported as promising candidates for enhancing the photocatalytic activity. In general, Ag nanoparticles are more attractive as dopants compared to other noble metals because of their high electrical and thermal conductivity, non-toxicity, cost-effectiveness, and high work function (Kadam et al., 2018). Kusdianto et al. (2017) reported that the addition of Ag nanoparticles enhanced the photocatalytic activity of the nanocomposite produced by up to 35% compared to pristine TiO₂ because Ag can be used as an electron acceptor to inhibit the electron-hole recombination.

ZnO-Ag nanocomposite can be fabricated by liquid-phase methods using sol-gel, precipitation, electrodeposition, hydrothermal, and solvothermal approaches (Jianguo et al., 2017; Kadam et al., 2018; Vaiano et al., 2018; Liu et al., 2019). These methods are able to fabricate nanocomposite at ambient temperature and atmospheric pressure. However, the disadvantages of these processes are that they involve a large number of processing steps and then require further steps to remove any residue or impurities, as well as completely removing the solvent. Furthermore, gas-phase methods employing spray drying pyrolysis have been utilized to fabricate ZnO-Ag nanocomposite (Dermenci et al., 2014). These methods are suitable for obtaining particles in a single step. However, decomposition of the precursors occurs inside the tubular furnace, which requires a high electrical power source. Another one-step process using the gas-phase method and flame pyrolysis has also been reported as a good candidate for producing the particles due to high crystallinity of the nanoparticles produced. Moreover, it is not necessary to deal with the solvent after fabrication as it evaporates during decomposition inside the flame reactor (Tani et al., 2002). The high purity of the product, with a relatively narrow size distribution, is another advantage of this method (Kammler et al., 2001). In addition, many types of low-cost precursors can be used as sources (Solero, 2017).

In this study, preference has been given to the flame pyrolysis method, as the energy source of the flame can be generated by simple combustion between the fuel and oxidizer, meaning it is cost-effective. In previous studies, our group has successfully fabricated ZnO by the flame pyrolysis method, in which the morphology of the particles produced was significantly affected by the temperature of the flame (Widiyastuti et al., 2013; Widiyastuti et al., 2014). However, to the best of our knowledge, no studies have reported the effect of Ag content on ZnO-Ag nanocomposite prepared by flame pyrolysis and the characterization of the products for the photocatalytic activity. Inspired by this gap, the objective of this study is to investigate the effect of Ag loading on ZnO-Ag nanocomposite synthesized by the flame pyrolysis method and their photocatalytic performance under UV light irradiation. Methylene blue (MB) was used as the model organic pollutant because it is commonly used as a synthetic dye in the textile industry and is not easily biodegraded by nature (Kusrini et al., 2018). Furthermore, MB is a heterocyclic aromatic compound, which is toxic and highly dangerous to humans (Balu et al., 2018). Using MB as a model organic pollutant, we believe that the results obtained will provide valuable information on MB degradation efficiency to help solve the environmental issue, especially due to the liquid waste of organic pollutants.

2. METHODS

2.1. Material and Experimental Setup

Zinc acetate dihydrate ($\text{Zn}(\text{CH}_3\text{COO})_2 \cdot 2\text{H}_2\text{O}$), p.a. 99.5%, Merck), silver nitrate (AgNO_3 , Merck), methylene blue ($\text{C}_{16}\text{H}_{18}\text{ClN}_3\text{S}$, Merck), and distilled water were used as received as precursors. They were prepared by dissolving the zinc acetate in distilled water in a homogeneous process using a sonicator to prepare the ZnO 0.1 M concentration. Silver nitrate with different weights ranging from 0 to 20% wt (based on zinc acetate) were mixed with the prepared ZnO 0.1 M under sonication. The mixed precursor solution was then fed into an ultrasonic nebulizer (Omron) operated at 1.7 MHz.

The lab-made experimental apparatus used for the fabrication of the ZnO-Ag nanocomposites through flame pyrolysis was similar to that of our previous study (Widiyastuti et al., 2014). However, some modifications were made by installing a peristaltic pump to pump the fresh precursor continuously into a nebulizer chamber. Through this modification, the volume of precursor inside the nebulizer could be controlled and kept constant during the nebulizing process in order to obtain similar precursor concentrations. An ultrasonic nebulizer was used to generate droplets by atomizing the precursor solution. The droplets produced by the nebulizer were then carried into the flame reactor by compressed air at a flow rate of 3 LPM. Before used, the compressed air was passed through silica gel to remove the moisture content from the air. Liquefied petroleum gas (LPG, commercial grade, PT. Pertamina) was used as fuel, and the compressed air was used as the oxidizer. Combustion reaction occurred in the premixed burner. The flow rate of LPG and oxidizer was kept constant at 0.3 and 2.8 LPM respectively. The precursor of mixed zinc acetate and silver nitrate was decomposed inside the flame reactor to produce ZnO-Ag nanocomposites. These were collected in the electrostatic precipitator, where the temperature was kept constant at 120°C in order to avoid condensation. Moreover, non-condensable gas was attracted by a vacuum pump and trapped in the water trap.

2.2. Characterizations

The crystalline phase and crystallite size of the nanocomposites produced were analyzed by X-ray diffraction (XRD, X'pert Philips) operated at an accelerating voltage of 40 kV and 30 mA using a $\text{CuK}\alpha$ radiation source ($\lambda = 0.15418$ nm). A scan speed of 10°/min and a sampling point of 0.02° were also used during this measurement. The surface morphology of the fabricated nanocomposite was observed by scanning electron microscopy (SEM, S-5200, Hitachi High Technologies). The samples were subjected twice to a carbon-based ion sputtering device for 1 min before observation by the SEM to eliminate the charging effect during analysis. The particle size distribution was estimated by measuring several hundred samples using ImageJ software. Furthermore, nitrogen adsorption-desorption (Autosorb-1, Quantachrome Instruments) experiments were conducted to analyze the Brunauer-Emmett-Teller (BET) specific surface area and the pore volume of the nanocomposites produced. The samples were degassed at 150°C prior to nitrogen adsorption-desorption measurements. The relative pressure (P/P_0) adsorption data, ranging from 0.05 to 0.3, was used to determine the BET surface area based on a multipoint BET method.

The photocatalytic activity of the ZnO-Ag nanocomposite was estimated by measurement of the photocatalytic degradation of an MB aqueous solution under UV light irradiation at room temperature. 6 mg of the ZnO-Ag nanocomposite was dispersed in 60 ml of MB solution. The suspensions, 6 mg ZnO-Ag dispersed in 60 ml MB solution, were stirred for 30 min in the dark chamber before irradiation to attain adsorption-desorption equilibrium. They were then exposed to the UV light irradiation under magnetic stirring. Sampling was carried out at 15 min intervals, when 4 ml suspension was taken and centrifuged. The MB concentration before and after irradiation was measured by UV-vis spectrophotometry (V-650, Jasco). The absorbance of the MB was determined by UV-vis spectrophotometry with a UV absorbance at 664 nm, primarily

originating from the MB. Subsequently, the concentration of MB was obtained by converting the absorbance values of the samples into MB concentrations based on an MB calibration curve (MB absorbance = $0.2053 \times$ MB concentration (mg/L)).

3. RESULTS AND DISCUSSION

Figure 1 shows the XRD patterns of the fabricated ZnO-Ag nanocomposites with different Ag content, including the pristine ZnO.

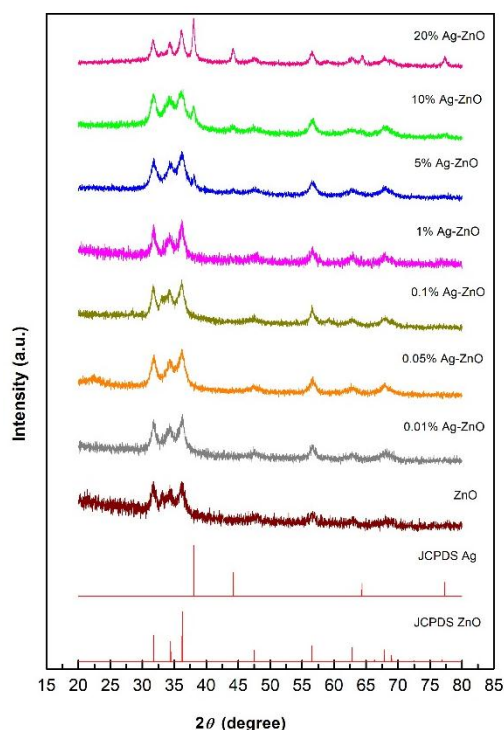


Figure 1 XRD patterns of ZnO-Ag nanocomposites with different Ag content, ranging from 0 to 20 %wt, prepared by flame pyrolysis.

It can be seen from Figure 1 that ZnO can be successfully fabricated by flame pyrolysis, as indicated by the diffraction peaks at 31.7° , 34.4° , 36.2° , 47.5° , 56.6° , 62.9° , and 68.0° which correspond to (100), (002), (101), (102), (110), (103) and (112) planes, respectively (Vaiano et al., 2017). Referring to Joint Committee on Powder Diffraction Standards (JCPDS), all the samples fabricated by this method have the typical hexagonal Wurtzite structure, which is the most stable ZnO structure. On the other hand, the XRD patterns also indicate that the nanocomposites produced have high crystallinity. Maximum diffraction intensity was observed at 36.2° . Four additional diffraction peaks, at 38.1° , 44.3° , 64.4° and 77.5° , are also shown in Figure 1 when the concentration of Ag is greater or equal to 5 %wt. These peaks correspond to (111), (200), (220) and (300) crystal planes respectively, due to the presence of Ag in the ZnO-Ag nanocomposite (Vaiano et al., 2017).

Figure 1 also shows an increase in the Ag peaks with increasing Ag content. It is clearly observed that the intensity of diffraction peaks at 38.1° , 44.3° , 64.4° and 77.5° is enhanced significantly by an Ag content of 20 %wt compared to other content levels. This difference is caused by increasing Ag content in the ZnO-Ag nanocomposite. Ag nanoparticles may be embedded in the ZnO surface, resulting in higher intensity. Another possibility may be the aggregation of Ag nanoparticles, forming an Ag cluster in the ZnO structure, which enhanced the intensity of the scanning sample. This possibility is in line with with the BET surface area result, which indicates

that the Ag content at 20 %wt showed the smallest surface area (see Table 1). Unexpectedly, Ag peaks are not observed when the concentration of Ag is less than 5 %wt. This can be attributed to the low concentration of Ag distributed uniformly in the ZnO-Ag nanocomposite. The average crystallite size (D) was calculated by the Scherrer equation (Equation 1), based on the highest intensity from the XRD patterns shown in Figure 1, using the same equation as in previous studies (Widiyastuti et al., 2013; Vaiano et al., 2017):

$$D = \frac{k \lambda}{B \cos \theta} \quad (1)$$

where k , λ , B , and θ are the constant (0.9), the wavelength of the X-ray source ($\lambda = 0.15418$ nm), the full-width at half-maximum corresponding to the XRD peaks, and the peak angle, respectively. Estimation of crystallite size using the Scherrer equation indicated that it was not significantly affected by the Ag content, and was found to be in the range of 2-9 nm (see Table 1). Yu et al. (2005) and Liu et al. (2019) also report that the crystallite size of TiO₂-Ag nanocomposite did not change significantly after adding Ag dopant; however, the addition of Ag decreased the phase transformation temperature. The highest Ag content (20 %wt) showed the largest crystallite size, as high as 9 nm, while the crystallite size with Ag loading of 0.1 %wt was the smallest. Because the difference in crystallite size is a matter of just a few nm, it can be assumed that such a difference may have a less significant effect on photocatalytic performance.

Table 1 Crystallite size, pore diameter, and specific surface area of ZnO-Ag nanocomposites with differing Ag content

Ag content (%)	Crystallite size ^a (nm)	Pore diameter ^b (nm)	Specific surface area ^b (m ² /g)
0	3.3	4.5	237.1
0.1	2.4	1.9	461.2
1	5.6	2.6	409.4
5	5.7	5.7	280.1
20	9.1	4.8	189.9

^aCrystallite size was estimated by the Scherrer equation (Equation 1)

^bPore diameter and specific surface area were calculated from the nitrogen adsorption–desorption BET measurement

Table 1 also shows the pore diameter and specific surface area of the ZnO-Ag nanocomposites with different concentrations of Ag. There is no significant trend in pore diameter with regard to Ag content, with the largest pore diameter obtained at an Ag content of 5 %wt. At the same time, the specific surface area increased after the addition of Ag 0.1 %wt, then decreased with increasing Ag content. The addition of Ag nanoparticles at 0.1 %wt resulted in the largest surface area. This can be attributed to the uniform distribution of particles, with less agglomeration (see SEM images in Figure 2). On the other hand, Ag nanoparticles are able to suppress the growth of ZnO particles. Yu et al. (2005) report that additional Ag content at certain concentrations increased the surface area. Table 1 also shows that the surface area decreased with increasing Ag content after the 0.1 %wt level. This decreasing surface area can be attributed to the agglomeration of particles with a high concentration of Ag content. This agrees well with the previous result, that the addition of Ag up to 3 %mol to the ZnO increased the surface area, but that this decreased when increasing the Ag content from 3 to 8 %mol (Liu et al., 2019).

Figure 2 shows SEM images of the morphology of the ZnO-Ag nanocomposites with different Ag content, including the pristine ZnO; in general, they have a spherical shape. It is also clearly observed that the morphology of the nanocomposite produced was not significantly different with

various Ag loadings. This result is in line with the results reported by Kusdianto et al. (2017). However, some aggregate particles can be observed from the SEM images, especially for the pristine ZnO and ZnO-Ag with a higher concentration of Ag content. Based on the SEM images shown in Figure 2, the aggregation of particles can be attributed to the high concentration of particles present in the gas stream when passing through the flame pyrolysis reactor, creating the possibility of the particles colliding with each other.

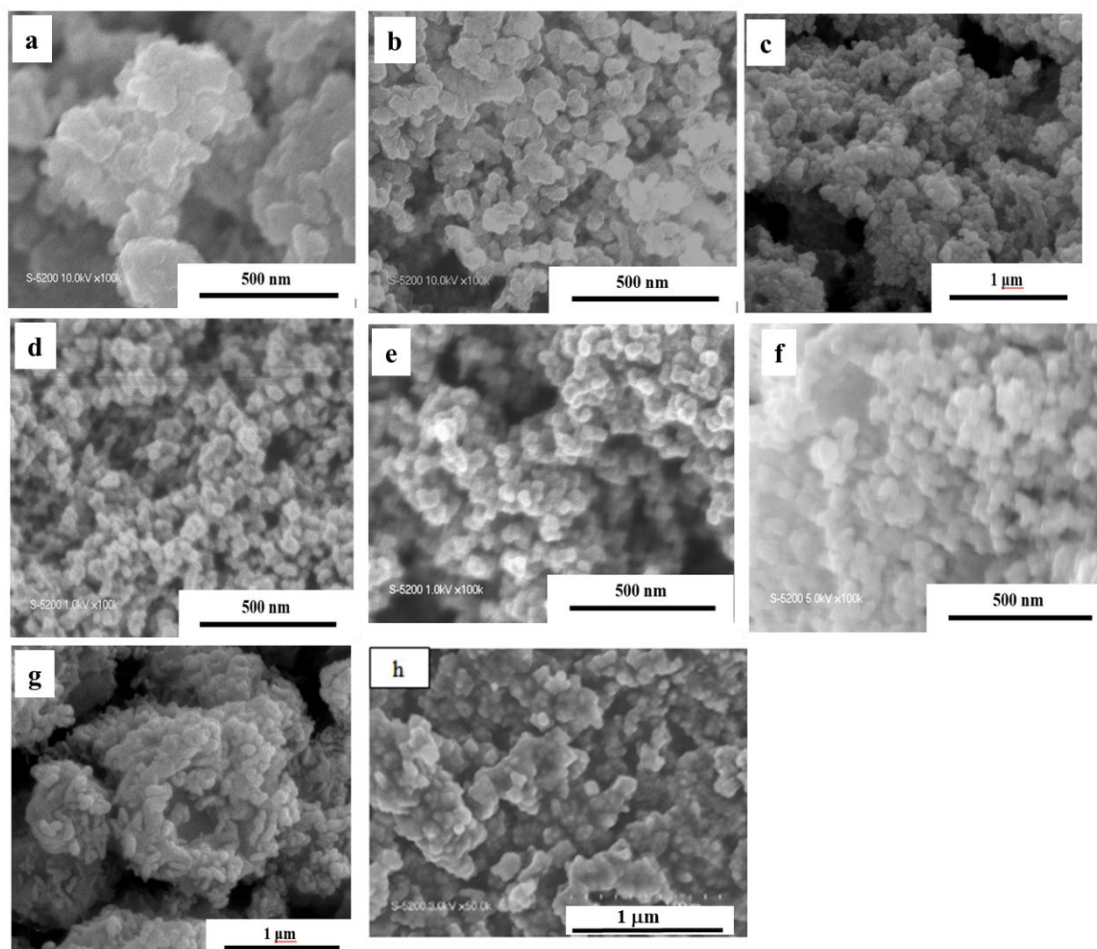


Figure 2 SEM images of ZnO-Ag nanocomposites prepared by flame pyrolysis at different Ag content levels: (a) 0 %; (b) 0.01 %; (c) 0.05 %; (d) 0.1 %; (e) 1 %; (f) 5 %; (g) 10 %; and (h) 20%

The particle size distribution was then estimated by measuring several hundred particles based on the SEM images using ImageJ software. Figure 3 shows that particle size increased slightly with increasing Ag content, with the exception of an Ag content of less than 1 %wt. This may be caused by the interaction of particles through the van der Waals force, which causes the molecules to interact and bond with each other. Our results are in a good agreement with those of Dehimi et al. (2015), which showed that the particle size of ZnO increased when Ag dopant was added to the ZnO particles during annealing, at a temperature of 500°C. Kusdianto et al. (2017) also report that particle size increased after adding the Ag nanoparticles to the TiO₂ matrix due to the metal-induced crystallization phenomenon and the coalescence of particles. Furthermore, the heat transfer among the ZnO may be enhanced by the presence of Ag nanoparticles.

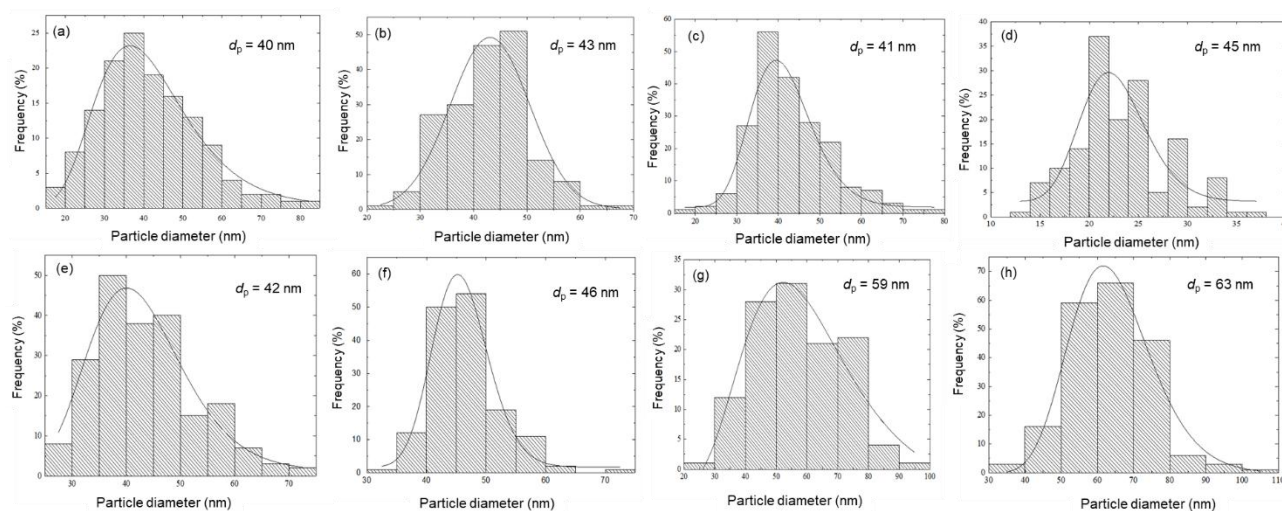


Figure 3 Particle size distribution of the ZnO-Ag nanocomposite estimated by measurement of the particles using imageJ at different Ag content levels of: (a) 0%; (b) 0.01%; (c) 0.05%; (d) 0.1%; (e) 1%; (f) 5%; (g) 10%; (h) 20%

Finally, photocatalytic activity was evaluated by measuring the MB degradation efficiency (*MDE*) under UV light irradiation with the following equation (Kusdianto et al., 2018):

$$MDE = \frac{(C_0 - C_t)}{C_0} \times 100\% \quad (2)$$

where C_0 and C_t correspond to the initial concentration of MB and after irradiation at a certain time (t), respectively. The nanocomposite samples were first subjected to dark conditions for 30 min under agitation before irradiation with UV light in order to attain adsorption-desorption equilibrium. The degradation efficiency of MB only reached 6% without irradiation with the UV light (UV light turned off) (see Figure 4). This indicates that the photocatalytic process is more dominant compared to the adsorption of ZnO. It is well known that one of the applications of ZnO is as use as an adsorbent.

It can be clearly observed in Figure 4 that the maximum degradation efficiency of MB using pristine ZnO can reach 25%. However, the degradation of MB increased with increasing Ag content. The maximum degradation efficiency of up to 65% was attained when an Ag content of 5%wt was used. Figure 4 also shows that the MB degradation efficiency decreased after increasing the Ag content to 10 and 20 %wt. This indicates that the optimum condition for MB degradation was reached when the Ag content was 5%wt, which can be attributed to the synergetic effect between the generation of electrons-holes by ZnO after UV light irradiation and the presence of Ag nanoparticles. In this case, the electrons placed in the conduction band (CB) will be immediately absorbed by a sufficient amount of Ag nanoparticles, because Ag is an electron acceptor (Yu et al., 2005; Kusdianto et al., 2017). On the other hand, the electrons trapped in the Ag nanoparticles could not return to the ZnO structure because the Fermi level of the ZnO is greater than that of Ag. Numerous holes in the valence band (VB) reacted with water or hydroxyl to produce hydroxyl radicals without any interferences from electron-hole recombination. Because the electrons produced are transferred to Ag nanoparticles, the electrons and holes are separated by this synergetic effect to give the fastest MB photodegradation. However, the degradation of MB is inhibited by electron-hole recombination in the absence of Ag or with a low content of Ag nanoparticles in the ZnO-Ag nanocomposites. Moreover, the degradation of MB decreased after increasing the Ag dopant to 10 and 20%wt, which can be

attributed to the large number of Ag nanoparticles blocking the incoming light to the ZnO nanoparticles, thus reducing the MB photoreaction.

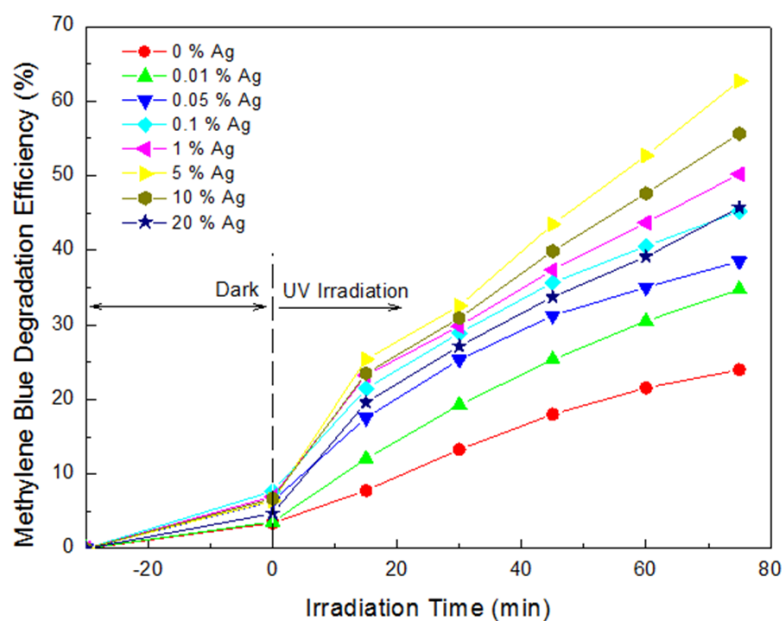


Figure 4 Methylene blue degradation efficiency of ZnO-Ag nanocomposite with different Ag content levels versus irradiation time

Photocatalytic performance was then determined by measurement of the pseudo-first-order rate constant (k), based on the equation $\ln(C_t/C_0) = kt$, as shown in Figure 5. The results obtained reveal that photocatalytic performance improved by increasing Ag content to 5%wt, but then decreased after increasing the Ag content to 10 and 20%wt. The lowest photocatalytic performance was obtained with the pristine ZnO, without adding Ag nanoparticles.

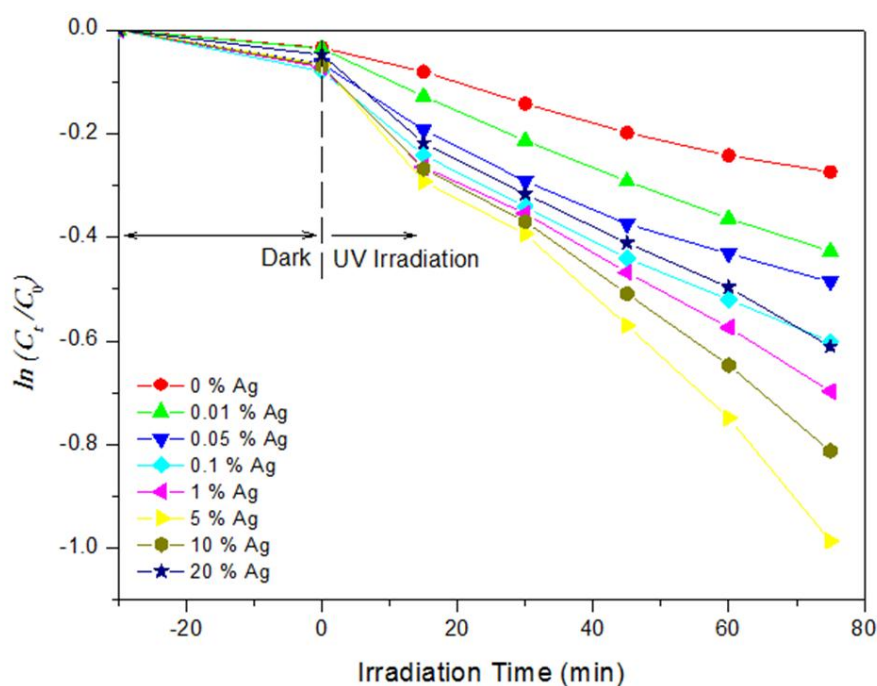


Figure 5 Plots of $\ln C_t/C_0$ vs irradiation time of the ZnO-Ag nanocomposites with various Ag loadings.

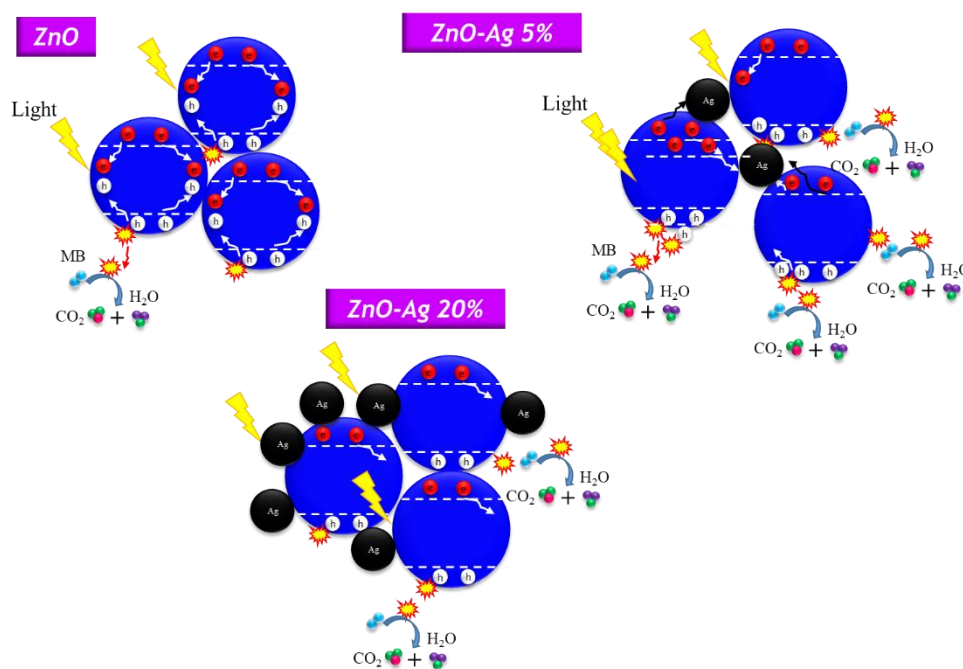


Figure 6 Illustration of the proposed mechanism of photocatalytic activity of ZnO-Ag nanocomposites with various Ag content levels under UV light irradiation.

In general, the photocatalytic activity is influenced by many parameters, such as the crystallinity, crystallite size, particle size, pore diameter, specific surface area, the existence or presence of dopant, morphology, and structure of the particle, among others. In this case, we can neglect the effect of crystallite size, as well as the crystallinity of the nanocomposites, because the results obtained show no significant difference between them. We may also disregard the results based on pore diameter for photocatalytic activity, because no conclusion can be reached regarding this tendency. However, we believe that the most important determiner of photocatalytic performance in this study is the existence of Ag nanoparticles. We propose the photocatalytic mechanism with differing Ag content, as illustrated in Figure 6. The mechanism for the photocatalysis of an organic compound by ZnO is initiated by the generation of electron-hole pairs when the photon energy of light is greater than or equal to that of the band gap energy. The electrons are promoted from the valence band (VB) to the conduction band (CB), leaving a hole in the VB. The holes generated in the VB will react with water or hydroxyl groups, forming hydroxyl radicals. These radicals enable the degradation of organic materials via oxidation. On the other hand, the electrons generated are attracted to Ag nanoparticles or react with oxygen, forming oxygen radicals. In this study, the lowest photocatalytic activity was obtained when using pristine ZnO (see Figure 5). This can be attributed to electron-hole recombination (see Figure 6). However, photocatalytic activity increased after adding Ag nanoparticles to ZnO matrix, which was caused by the migration of electrons to the Ag nanoparticles, as the Ag particles serve as an electron trap, reducing the recombination of electrons and holes (Kusdianto et al., 2017). Unfortunately, photocatalytic activity decreased after adding the Ag dopant at levels of 10 and 20 wt%. This may have been due to the agglomeration of Ag particles, which blocked the penetration of light, resulting in decreased photocatalytic performance.

4. CONCLUSION

ZnO-Ag nanocomposites have been successfully fabricated by a one-step process using flame pyrolysis. The effect of Ag content on the nanocomposites was also investigated. The XRD results indicate that the ZnO produced by flame pyrolysis has a typical hexagonal Wurtzite

structure with high crystallinity. The existence of Ag in the nanocomposite could be detected by XRD when the Ag content was greater or equal to 5%wt. The crystallite size of the nanocomposites was not significantly changed by varying the Ag content. The spherical shape of the ZnO, with some agglomeration of particles, was observed by SEM analysis, while particle size increased slightly with increasing Ag content. However, pore diameter did not show any clear tendency with the various Ag loadings, whereas the surface area increased to 0.1% wt, then decreased with increasing Ag content. Finally, photocatalytic activity evaluated by measuring MB degradation under UV light irradiation showed that maximum degradation efficiency of 63% could be achieved when Ag content of 5 %wt was used. The best photocatalytic activity was attained at 5%wt of Ag. We believe that this finding provides valuable information for the fabrication method of ZnO-Ag nanocomposite, as well as the effect of Ag content, with wide future applicability in various fields such as dye-sensitized solar cells, gas sensors, antibacterial applications, and photocatalysis.

5. ACKNOWLEDGEMENT

The authors are grateful to Herlinda S., Ika Silvia A., and Nurul Ika for their assistance in the experiments. They would also like to thank Mr. Jiang D. and M. Ishihara for their assistance in the SEM observation. This work was financially supported by the Direktorat Riset dan Pengabdian Masyarakat (DRPM) DIKTI, with contract grant No. 955/PKS/ITS/2018.

6. REFERENCE

- Balu, S., Uma, K., Pan, G.T., Yang, T.C., Ramaraj, S.K., 2018. Degradation of Methylene Blue Dye in the Presence of Visible Light using $\text{SiO}_2@ \alpha\text{-Fe}_2\text{O}_3$ Nanocomposites Deposited on SnS_2 Flowers. *Materials*, Volume 11(6), pp. 1030:1–17
- Chatterjee, D., Dasgupta, S., 2005. Visible Light Induced Photocatalytic Degradation of Organic Pollutants. *Journal of Photochemistry and Photobiology C: Photochemistry Reviews*, Volume 6(2-3), pp. 186–205
- Dehimi, M., Touam, T., Chelouche, A., Boudjouan, F., Djouadi, D., Solard, J., Fischer, A., Boudrioua, A., Doghmane, A., 2015. Effects of Low Ag Doping on Physical and Optical Waveguide Properties of Highly Oriented Sol-gel ZnO Thin Films. *Advances in Condensed Matter Physics*, Volume 2015, Article ID 740208, pp. 1–10
- Dermenci, K.B., Genc, B., Ebin, B., Olmez-Hanci, T., Gürmen, S., 2014. Photocatalytic Studies of Ag/ZnO Nanocomposite Particles Produced via Ultrasonic Spray Pyrolysis Method. *Journal of Alloys and Compounds*, Volume 58, pp. 267–273
- Duan, X., Wang, G., Wang, H., Wang, Y., Shen, C., Cai, W., 2010. Orientable Pore-size-distribution of ZnO Nanostructures and Their Superior Photocatalytic Activity. *CrystEngComm*, Volume 12(10), pp. 2821–2825
- Jianguo, L., Zhu, Q., Zeng, Z., Zhang, M., Yang, J., Zhao, M., Wang, W., Cheng, Y., He, G., Sun, Z., 2017. Enhanced Photocurrent and Photocatalytic Properties of Porous ZnO Thin Film by Ag Nanoparticles. *Journal of Physics and Chemistry of Solids*, Volume 111, pp. 104–109
- Kadam, A.N., Bhopate, D.P., Kondalkar, V.V., Majhi, S.M., Bathula, C.D., Tran, A.V., Lee, S.W., 2018. Facile Synthesis of Ag-ZnO Core-shell Nanostructures with Enhanced Photocatalytic Activity. *Journal of Industrial and Engineering Chemistry*, Volume 61, pp. 78–86
- Kammler, H.K., Madler, L., Pratsinis, S.E., 2001. Flame Synthesis of Nanoparticles. *Chemical Engineering and Technology*, Volume 24(6), pp. 583–596

- Kusdianto, K., Jiang, D., Kubo, M., Shimada, M., 2017. Fabrication of TiO₂-Ag Nanocomposite Thin Films Via One-step Gas-phase Deposition. *Ceramics International*, Volume 43(6), pp. 5351-5355
- Kusdianto, K., Jiang, D., Kubo, M., Shimada, M., 2018. Effect of Annealing Temperature on the Photocatalytic Activity of Ag-TiO₂ Nanocomposite Films by One-step Gas-phase Deposition. *Materials Research Bulletin*, Volume 97, pp. 497-505
- Kusrini, E., Wicaksono, B., Yulizar, Y., Prasetyanto, E.A., Gunawan, C., 2018. Textile Dye Removal from Aqueous Solution using Modified Graphite Waste/Lanthanum/Chitosan Composite. *In: IOP Conference Series: Materials Science and Engineering*, Volume 316, pp. 012029
- Liu, Y., Zhang, Q., Xu, M., Yuan, H., Chen, Y., Zhang, J., Luo, K., Zhang, J., You, B., 2019. Novel and Efficient Synthesis of Ag-ZnO Nanoparticles for the Sunlight-induced Photocatalytic Degradation. *Applied Surface Science*, Volume 476, pp. 632-640
- Mamat, M., Abdullah, M.A.A., Kadir, M.A., Jaafar, A.M., Kusrini, E., 2018. Preparation of Layered Double Hydroxides with Different Divalent Metals for the Adsorption of Methyl Orange Dye from Aqueous Solutions. *International Journal of Technology*, Volume 9(6), pp. 1103-1111
- Rahman, A., Nurjayadi, M., Wartilah, R., Kusrini, E., Prasetyanto, E.A., Degermenci, V., 2018. Enhanced Activity of TiO₂/Natural Zeolite Composite for Degradation of Methyl Orange under Visible Light Irradiation. *International Journal of Technology*, Volume 9(6), pp. 1159-1167
- Solero, G., 2017. Synthesis of Nanoparticles through Flame Spray Pyrolysis: Experimental Apparatus and Preliminary Results. *Nanoscience and Nanotechnology*, Volume 7(1), pp. 21-25
- Tani, T., Madler, L., Pratsinis, S.E., 2002. Homogeneous ZnO Nanoparticles by Flame Spray Pyrolysis. *Journal of Nanoparticle Research*, Volume 4(4), pp. 337-343
- Vaiano, V., Matarangolo, M., Murcia, J.J., Rojas, H., Navío, J.A., Hidalgo, M.C., 2018. Enhanced Photocatalytic Removal of Phenol from Aqueous Solutions using ZnO Modified with Ag. *Applied Catalysis B: Environmental*, Volume 255, pp. 197-206
- Vaiano, V., Matarangolo, M., Sacco, O., Sannino, D., 2017. Photocatalytic Removal of Eriochrome Black T Dye Over ZnO Nanoparticles Doped with Pr, Ce or Eu. *Chemical Engineering Transactions*, Volume 57, pp. 625-630
- Widiyastuti, W., Machmudah, S., Nurtono, T., Winardi, S., 2013. Effect of the Flame Temperature on the Characteristics of Zirconium Oxide Fine Particle Synthesized by Flame Assisted Spray Pyrolysis. *In: AIP Conference Proceedings*, Volume 1554, pp. 150-153
- Widiyastuti, W., Maula, I., Nurtono, T., Taufany, F., Machmudah, S., Winardi, S., Panatarani, C., 2014. Preparation of Zinc Oxide/Silica Nanocomposite Particles via Consecutive Sol-gel and Flame-assisted Spray-drying Methods. *Chemical Engineering Journal*, Volume 254, pp. 252-258
- Winatapura, D.S., Dewi, S.H., Adi, W.A., 2016. Synthesis, Characterization, and Photocatalytic Activity of Fe₃O₄@ZnO Nanocomposite. *International Journal of Technology*, Volume 7(3), pp. 408-416
- Yu, J., Xiong, J., Cheng, B., Liu, S., 2005. Fabrication and Characterization of Ag-TiO₂ Multiphase Nanocomposite Thin Films with Enhanced Photocatalytic Activity. *Applied Catalysis B: Environmental*, Volume 60(3-4), pp. 211-221